JOURNAL OF MECHANICS OF CONTINUA AND MATHEMATICAL SCIENCES
www.journalimcms.org

ISSN (Online) : 2454 -7190 Vol.-17, No.-2, February (2022) pp 1-14 ISSN (Print) 0973-8975

ANALYSIS OF RACETRACK RESONATOR USING SIGNAL PROCESSING TECHNIQUE

Sabitabrata Dey

Dept. of Applied Electronics & Instrumentation Engineering,
College of Engineering & Management, Kolaghat. West Bengal

sb_dey@rediffmail.com.

https://doi.org/10.26782/jmcms.2022.02.00001

(Received: November 10, 2021; Accepted:January 18, 2022)

Abstract

Optical double racetrack resonator (ODRR) and optical quadruple racetrack resonator (OQRR) made of Silicon-on-insulator (SOI) with their effective refractive indices changing with respect to frequency have been analyzed for obtaining optical filter with wider ranges of free spectral range (FSR). FSR expansion is based on the Vernier principle. Delay line signal processing in Z- domain and Mason's gain formula is being used for analyzing these ODRR and OQRR. A free spectral range of 4.87THz is obtained for the drop port. Further, the change in the dimensions of the racetrack resonators produced an enhanced FSR of 5.77THz for ODRR. Combining both this model of ODRR we obtained an OQRR model that produces FSR as much as 6.86THz. Apart from obtaining wider FSR, this architecture exhibits interstitial spurious transmission of almost -50dB with negligible resonance loss. Group delay, dispersion characteristics, and finesse have also been determined for the architecture.

Keywords: Racetrack resonator, Mason's gain formula, free spectral range, Vernier principle, Resonance loss, Group delay, Dispersion.

I. Introduction

Optical racetrack resonators based on evanescent-field are a wide range of passive elements for the selection of the wavelength which play a vital role in the field of integrated optics. Increasing demand for data bandwidth has resulted in cost-effective devices within the electronic chips of high-performance computing or commercial communication systems like dense wavelength division multiplexing (DWDM) applications[XI, VII, VI, XVIII]. Add-drop filters made of racetrack resonator can also be utilized as graphene-based nano-photonic devices which is preferable for its use in terahertz and infrared ranges [I]. Hence an optical quadruple racetrack resonator (OQRR) along with ODRR plays a vital role in this regard. The unique characteristics of these resonators are that they find applications in converters, filters, isolators, delay lines, etc. These racetrack resonators can also be used for obtaining logic gates [XII] or memory devices. Here, in this work, we present the method of analysis and synthesis of double and quadruple racetrack resonator configurations using the *Vernier principle* in the Z-domain. The material used here Silicon-on-Insulator (SOI) with a higher relative refractive index difference, which

provides flexibility in device miniaturization. Currently, photonic devices on SOI substrates are being extensively investigated worldwide [VII]. The microresonators, fabricated using silicon-on-insulator (SOI) platforms [VI, XVIII, I], exhibit a great potential to build space, power, and spectrally efficient on-chip photonic networks that is compatible with CMOS electronics. Apart from the above advantages, optical cavities on SOI and resulting racetrack resonators are highly attractive, because it is simpler to design the parallel couplers region than in a ring resonator with the possibility to achieve high-quality factors (Q) and reduce the stress on the coupler region [XII]. This racetrack resonator also plays a prominent role to reduce the congestion problem in the busy switches [VIII]. The ODRR and OQRR elaborated in this literature, combine the advantages of high-density electronics and high-speed photonics which gives significant enhancement in performance, cost-effectiveness compared to similar kinds of other architectures.

II. Mathematical Background and Modeling Methodology

Racetrack resonators are comprised of straight waveguide sections with semi-circular segments. Here in these architectures, such racetrack resonators with the same straight section lengths and of different radii both for ODRR and OQRR have been used. Their straight sections of lengths L and with semicircular portions of radii R_1 and R_2 for ODRRs and R_1, R_2, R_3, and R_4 for OQRR respectively are shown in Fig 1(a). Two racetracks for ODRR and four such racetrack resonators for OQRR are serially coupled with straight bus waveguides from where the optical signal inputted and outputted from are named input and output waveguides. The straight and racetrack portions are coupled with each other using directional optical couplers of coupling coefficients k_1, k_2, k_3, k_4, and k_5 respectively for OQRR. Fig. 1(b) represents the z-transform equivalent of an OQRR structure which is known as a *signal flow graph*.

Here, in this article, we have considered that the refractive index of the SOI material is changing concerning frequency which can be expressed as [VII],

$$n_g = n_e(f_0) + f_0 \frac{dn_e}{df} \tag{1}$$

where $f = f_0$; f_0 being the center frequency; n_e is the effective refractive index and n_g is the group refractive index.

When two optical waveguides are closely coupled using a directional optical coupler both at the input and output, evanescent field coupling occurs. The transfer matrix of such configuration can be expressed by a 2×2 matrix or chain matrix formulation [V],

$$\begin{bmatrix} E_1^0 \\ E_2^0 \end{bmatrix} = Q \begin{bmatrix} C & -jS \\ -jS & C \end{bmatrix} e^{jkL_C} \begin{bmatrix} E_1^i \\ E_2^i \end{bmatrix} \tag{2}$$

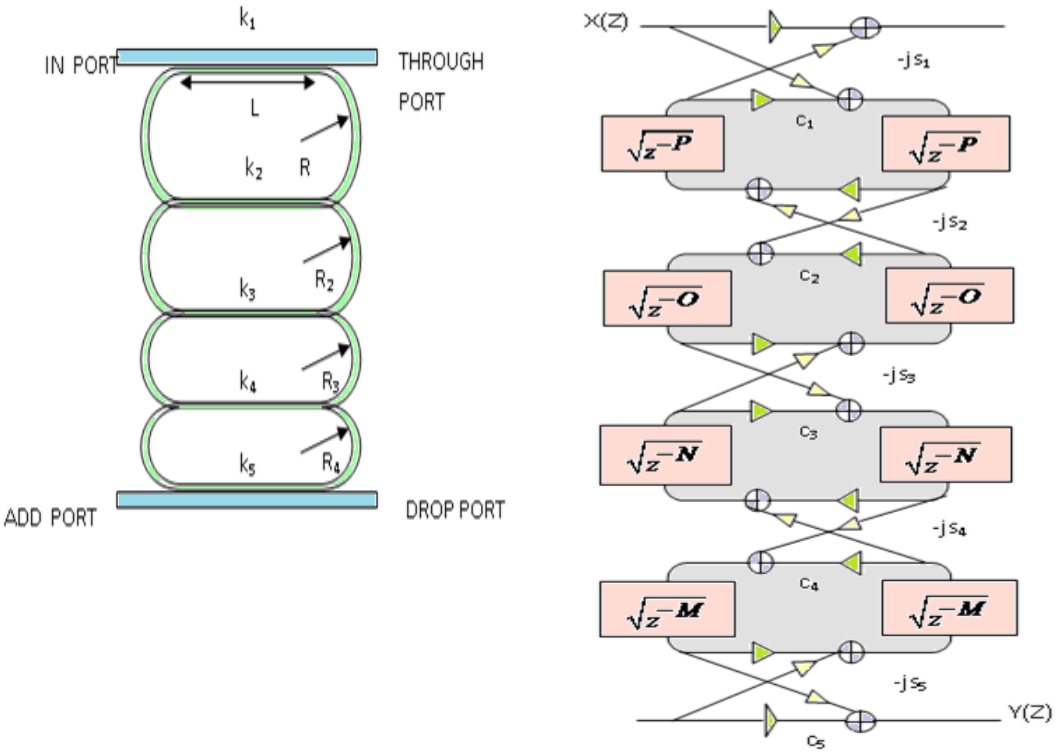

(a) (b)

Fig 1. (a) : Optical quadruple racetrack resonator (OQRR); (b) z-transformation equivalent (*Signal Flow Graph*) of (a).

where E_1^o and E_2^o represents coupler at the output region. E_1^i and E_2^i denotes coupler at the input region. Here *k* is the propagation constant and L_C is the effective length of the coupling region in between two racetrack resonators. Here C and S are the cross and self-coupling coefficients respectively which describe the interaction intensity between two closely coupled resonators. Q is the overall amplitude transmission coefficient where Q lies in between 0.9 and 1.

This racetrack ODRR and OQRR architectures have been analyzed using the delay line signal processing technique and Mason's gain formula [XV]. The backbone of this model is to modulate the *unit delay*. Here unit delay time is being represented by [III],

$$T_i = 2n_g(L_{ui} + \pi R_i)/c \qquad (3)$$

Here, n_g is the group refractive index of the waveguide material. The term within the parenthesis represents the racetrack half-perimeter length and *c* is the velocity of light, where, L_{ui} is the length of the straight portion of the racetrack resonator and R_i is the radius of the semi-circular portion racetrack resonators. The total delay is

the integer multiple of this *unit delay*. The frequency response of such a racetrack resonator is generally periodic and one such period of that frequency response is called *free spectral range* (FSR). Hence the relationship between FSR and unit delay is expressed as,

$$FSR_i = 1/T_i = c/2n_g(L_{ui} + \pi R_i). \tag{4}$$

It can be seen that the *free spectral range* of the racetrack resonator is inversely proportional to the total length is the straight portion added with the curved portion of the resonator that is shown in equation (4). Thus for obtaining higher ranges of FSR, the length of the resonator must be reduced. Minimizing the total length would maximize the FSR but it can be done up to a certain limit. If the radius of curvature or the effective ring length is shortened much then the banding loss will increase exponentially [VI]. For mitigating these bending losses without compromising the obtainable FSR of the racetrack resonator, a proper designing method has to be obtained. The difference in the performance of ODRR and OQRR by using waveguides of high refractive indices difference materials like silicon-on-insulators (SOI) has been observed in this work.

Vernier principle has been used here for obtaining extended FSR utilizing series coupling multiple racetrack resonators for both the architectures. Here two such racetrack resonators for ODRR and four such racetrack resonators for OQRR with different path lengths and two straight bus waveguides have been used.

Hence for enhancing the interaction between the two input and output access waveguides and the resonators, the distances between the waveguides and the resonators have to be reduced up to a certain limit. when the resonators have the air gap width between the waveguide path and the resonator is small enough then the mode conversion losses in between interconnecting paths cannot be neglected. Hence the assumption made in the case of circular ring resonator-based devices that is $S_i^{\,2} + C_i^{\,2} = 1$ does not hold good for this racetrack type resonators where the interconnection regions are wider [XVI].

Vernier principle is used to enhance the FSR of the racetrack resonator here. Accordingly, extended FSR can be written as [XVI],

$$FSR_{Extended} = MFSR_1 = NFSR_2 = OFSR_3 = PFSR_4 \tag{5}$$

where M, N, O, and P are the co-prime numbers, called resonant numbers of corresponding racetrack resonators. FSR_1 is the free spectral range of the first racetrack resonator, FSR_2 is the free spectral range of the second racetrack resonator, and so on.

Since this is a linear time-invariant (LTI) system, the overall transfer function of this racetrack resonator is determined using Mason's gain formula [XV] which can be expressed as,

$$T_f = \frac{T_1\Upsilon_1}{\Upsilon} + \frac{T_2\Upsilon_2}{\Upsilon} + \ldots\ldots = \frac{\sum T_n\Upsilon_n}{\Upsilon} \tag{6}$$

where T_1 is the transmittance of the 1st forward path, similarly T_n is the transmittance of the nth forward path and Υ is the determinant of the graph and is expressed as,

$$\Upsilon = 1 - \sum L_1 + \sum L_2 - \sum L_3 + ... \tag{7}$$

where $\sum L_1$ is the sum of products of transmittance of all the individual closed loops of the signal flow graph, $\sum L_2$ is the sum of products of transmittance of all possible combinations of two non touching closed loops, and so on. All the loops and paths are calculated using the stated equations [XVII]. Eventually Υ becomes the value of the part which does not touch the forward path.

For drop port transfer function (ODRR),

$$\begin{aligned} T_i\Upsilon_i = T_1\Upsilon_1 &= (-jS_1\sqrt{z^{-M}})(-jS_2\sqrt{z^{-N}})\{-jS_3(1-0)\} \\ &= jS_1S_2S_3\sqrt{z^{-(M+N)}}\,. \end{aligned} \tag{8}$$

For drop port transfer function (OQRR),

$$\begin{aligned} T_1\Upsilon_1 &= (-jS_1\sqrt{z^{-M}})(-jS_2\sqrt{z^{-N}})(-jS_3\sqrt{z^{-O}})(-jS_4\sqrt{z^{-P}})\{-jS_5(1-0)\} \\ &= -jS_1S_2S_3S_4S_5\sqrt{z^{-(M+N+O+P)}} \end{aligned} \tag{9}$$

where,

$$j = \sqrt{-1}\,.$$

Since all the loops touch the forward path, $\Upsilon_1 = 1$

Thus, the Drop port transfer function for ODRR which uses the Vernier effect is given as,

$$T.F_{drop} = \frac{iS_1S_2S_3\sqrt{z^{-(M+N)}}}{1 - C_1C_2z^{-M} - C_2C_3z^{-N} + C_1C_3(S_2^2 + C_2^2)z^{-(M+N)}} \tag{10}$$

Two defining parameters of a racetrack resonator are effective perimeter length L and complex propagation constant (β−jα). Here β is phase constant and α is amplitude attenuation coefficient due to intrinsic loss mechanism of the cavity i.e., radiation and loss due to imperfection such as surface roughness. All the losses have been included in the round trip loss γ[XIV]. Considering ring losses and defining the resonant numbers M=4 and N=5 (from experimental results) and M=6 and N=7 (for getting wider FSR in case of ODRR), lastly combining them for having the OQRR from (4) for the extended value of FSR[XIII], the overall transmittance of this structure as a demonstration of the ODRR can be modified as follows,

$$T.F_{drop} = \frac{iS_1S_2S_3\gamma_1\gamma_2\sqrt{z^{-9}}}{1 - \gamma_1C_1C_2z^{-5} - \gamma_2C_2C_3z^{-4} + \gamma_1\gamma_2C_1C_3(S_2^2 + C_2^2)z^{-9}} \tag{11}$$

where γ_1 and γ_2 are the round trip losses of the racetrack1 and racetrack2 respectively.

Following the similar principle just discussed the through port transfer function which uses Vernier principle is given as (for ODRR),

$$T_1\Upsilon_1 = C_1(1 - C_1C_2z^{-M} - C_2C_3z^{-N})$$
$$T_2\Delta_2 = (-jS_1\sqrt{z^{-M}})(-jS_2\sqrt{z^{-N}})(C_3\sqrt{z^{-N}})(-jS_2\sqrt{z^{-M}})(-jS_1) = S_1^2S_2^2C_3z^{-(M+N)} \quad (12)$$

Here, $T_i\Upsilon_i = T_1\Upsilon_1 + T_2\Upsilon_2$.

$$T.F_{through} = \frac{C_1(1-\gamma_1C_1C_2z^{-5} - \gamma_2C_2C_3z^{-4}) + \gamma_1\gamma_2q^2S_1^{\,2}S_2^{\,2}C_3z^{-9}}{1-\gamma_1C_1C_2z^{-5} - \gamma_2C_2C_3z^{-4} + \gamma_1\gamma_2C_1C_3(S_2^2+C_2^2)z^{-9}} \quad (13)$$

where, $S_i = \sqrt{k_i}$ and $C_i = \sqrt{1-k_i}$.

Similarly, for OQRR the through port transfer function is based upon the Vernier principle as follows:

$$T_1\Upsilon_1 = C_1(1 - C_1C_2z^{-M} - C_2C_3z^{-N} - C_3C_4z^{-O} - C_4C_5z^{-P})$$
$$T_2\Upsilon_2 = (-jS_1\sqrt{z^{-M}})(-jS_2\sqrt{z^{-N}})(-jS_3\sqrt{z^{-O}})(-jS_4\sqrt{z^{-P}})(C_5\sqrt{z^{-P}})(-jS_4\sqrt{z^{-O}})(-jS_3\sqrt{z^{-N}})(-jS_2\sqrt{z^{-M}})(-jS_1)$$
$$= S_1^2S_2^2S_3^2S_4^2C_3z^{-(M+N+O+P)} \quad (14)$$

Similarly, the Transfer Function of the drop port for OQRR is as below,

$$T.F_{drop} = \frac{-jS_1S_2S_3S_4S_5\sqrt{z^{-(M+N+O+P)}}}{1-C_1C_2z^{-M}-C_2C_3z^{-N}-C_3C_4z^{-O}-C_4C_5z^{-P}+C_1C_3(S_2^2+C_2^2)z^{-(M+N)}+C_1C_2C_3C_4z^{-(M+O)}}$$
$$+\{C_2C_4(S_3^2+C_3^2)+C_1C_2C_4C_5\}z^{-(N+O)}+C_2C_3C_4C_5z^{-(N+P)}+C_3C_5(S_4^2+C_4^2)z^{-(O+P)}-\{C_1C_4C_2^2(S_3^2+C_3^2)+$$
$$C_1C_4S_2^2(S_3^2+C_3^2)\}z^{-(M+N+O)}-C_1C_3C_4C_5(S_2^2+C_2^2)z^{-(M+N+P)}-C_1C_2C_3C_5(S_4^2+C_4^2)z^{-(M+O+P)}$$
$$-\{C_2C_5S_4^2(S_3^2+C_3^2)+C_2C_5C_4^2(S_3^2+C_3^2)\}z^{-(N+O+P)}+\{C_1C_5S_2^2S_4^2(S_3^2+C_3^2)+C_1C_5C_4^2S_2^2(S_3^2+C_3^2)$$
$$+C_1C_5C_2^2S_3^2(S_4^2+C_4^2)+C_1C_5C_2^2C_3^2(S_4^2+C_4^2)\}z^{-(M+N+O+P)} \quad (15)$$

Transfer function of the through port for OQRR as below,

$$T.F_{through} = \frac{C_1(1-C_1C_2z^{-M} - C_2C_3z^{-N} - C_3C_4z^{-O} - C_4C_5z^{-P}) + S_1^2S_2^2S_3^2S_4^2C_5z^{-(M+N+O+P)}}{1-C_1C_2z^{-M} - C_2C_3z^{-N} - C_3C_4z^{-O} - C_4C_5z^{-P} + C_1C_3(S_2^2+C_2^2)z^{-(M+N)} + C_1C_2C_3C_4z^{-(M+O)}} \quad (16)$$
$$+\{C_2C_4(S_3^2+C_3^2)+C_1C_2C_4C_5\}z^{-(N+O)} + C_2C_3C_4C_5z^{-(N+P)} + C_3C_5(S_4^2+C_4^2)z^{-(O+P)}$$
$$-\{C_1C_4C_2^2(S_3^2+C_3^2)+C_1C_4S_2^2(S_3^2+C_3^2)\}z^{-(M+N+O)} - C_1C_3C_4C_5(S_2^2+C_2^2)z^{-(M+N+P)}$$
$$-C_1C_2C_3C_5(S_4^2+C_4^2)z^{-(M+O+P)} - \{C_2C_5S_4^2(S_3^2+C_3^2)+C_2C_5C_4^2(S_3^2+C_3^2)\}z^{-(N+O+P)}$$
$$+\{C_1C_5S_2^2S_4^2(S_3^2+C_3^2)+C_1C_5C_4^2S_2^2(S_3^2+C_3^2)+C_1C_5C_2^2S_3^2(S_4^2+C_4^2)+C_1C_5C_2^2C_3^2(S_4^2+C_4^2)\}z^{-(M+N+O+P)}$$

Considering the round trip delays the losses the above OQRRs drop port and through port transfer function can be written similarly.

II. Characteristics of Racetrack Resonator

(a) Group Delay

Group delay is defined as the rate of change of total phase shift concerning the angular frequency that is expressed as,

$$\tau_g = -\frac{d\phi}{d\omega} \tag{17}$$

where φ is the total phase shift and ω is the angular frequency.
Elaborately it can be expressed as a negative derivative of the phase of the transfer function for drop port in this work concerning angular frequency[III] and can be expressed as,

$$\tau_g = -\frac{d}{d\omega}\tan^{-1}\left[\frac{Imaginary\ part\ of\ \ Transfer\ function}{Real\ part\ of\ \ Transfer\ function}\right]_{z=\exp(j\omega)} \tag{18}$$

Here, the phase shift can be represented by taking an arctan of the ratio of the imaginary part to the real part of the transfer function. Group delay has been taken into account because it matters in the enhancement of the phase sensitivity and it can be normalized in terms of unit delay T. Hence absolute group delay can be defined as $\tau = T\tau_g$ and its unit is in seconds ranging in Picosecond.

(b) Dispersion

It causes widening of signal pulses near its resonant peaks as can be seen in Fig. 4(d). In this work structural dispersion is determined for quadruple optical racetrack architecture [XVI]. It is primarily rate of change of group delay stated above concerning the frequency and mathematically expressed as,

$$D = -\frac{d\tau_g}{d\omega} \tag{19}$$

where ω is the normalized angular frequency. In fiber-optic communication systems dispersion is defined as the derivative of group delay concerning wavelength. The dispersion of a racetrack resonator along with its total traversed path in a resonator can be written as,

$$D = -\frac{1}{Total\ Length\ of\ \ a\ Racetrack\ Resonator}\frac{d\tau_g}{d\lambda} \tag{20}$$

where $2(L_i + \pi R_i)$ is the total path length for a single racetrack, L_i and R_i are the lengths of the straight path and the radii of the semicircular path respectively.

(c) Finesse

Finesse is the performance indicator of a racetrack resonator. It is expressed as the ratio of free spectral range (FSR) to the full width at half maxima (FWHM) and denoted as F. It can be is expressed as [XIV],

$$F = \frac{Free\ Spectral\ range_{ODRR}}{Full\ Width\ at\ Half\ \ Maxima_{ODRR}} = \frac{Free\ Spectral\ range_{OQRR}}{Full\ Width\ at\ Half\ \ Maxima_{OQRR}} \tag{21}$$

Alternately, *Finesse* is proportional to the number of round-trip delays traversed before the light intensity in the micro ring racetrack resonator decays exponentially.

IV. Simulation Results

Frequency responses of the optical double racetrack resonator (ODRR) and quadruple racetrack resonator (OQRR) and group delay, dispersion characteristics for OQRR are computed and analyzed in the MATLAB platform. Silicon-on-insulator (SOI) with high refractive index difference has been used as constituent waveguide material to mitigate bending loss. Utilizing the delay line signal processing technique in Z-domain and Vernier principle we got the frequency response for ODRR that is similar to the experimental results [XIII]. We observed the free spectral range for ODRR as much as 4.87 THz for drop port transmittance only as shown in the following Fig. 2.

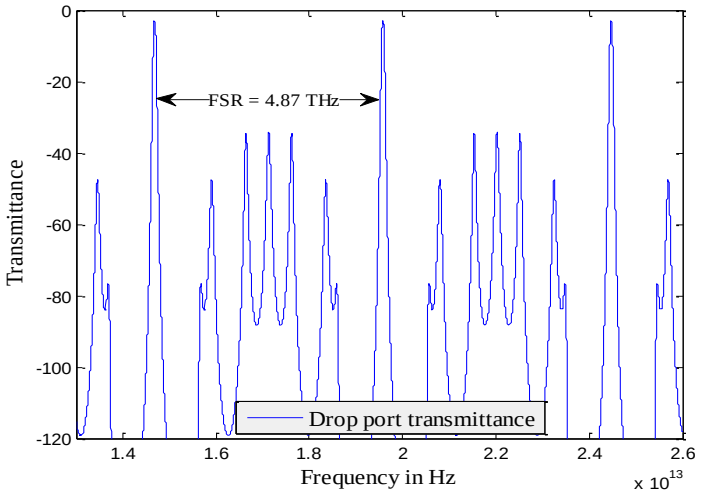

Fig. 2. Drop port transmittance compared with experimental drop port response with the same straight section in both the resonators as 15 µm along with their radius as 6.545 µm and 4.225 µm. The design parameters M = 5 and N=4 are the co-prime numbers. $k_1 = 0.36$, $k_2 = 0.024$ and $k_3 = 0.36$ respectively.

Following the same methodology, drop and through port responses with superior parameter is shown in Fig. 3. This architecture provides an FSR of 5.77THz.

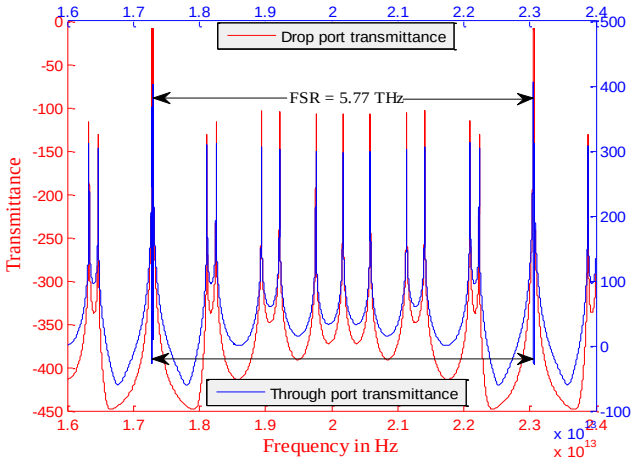

Fig 3. Drop port and through the port response of an ODRR with equal straight sections of 15 µm and radii of 6.76 µm and 8.68 µm here. O =7 and P = 6 respectively are the co-prime numbers. k_1 = 0.002, k_2 =0.001 and k_3 = 0.002 respectively.

Combining two such ODRR just discussed above, an OQRR is formed with equal straight sections in both the resonators as 15 µm and curved segments of radii as 4.225 µm, 6.545 µm, 6.76 µm, and 8.68 µm respectively. Assuming the design parameters, M =7, N = 6, O = 5 and P = 4 respectively as the co-prime numbers and k_1 = 0.06, k_2 = 0.08, k_3 = 0.095, k_4 = 0.08 and k_5 = 0.06 respectively the drop and through port responses are shown in Fig.4(a).
A zoom-in view of the single resonant peak of such OQRR is shown in Fig. 4(b) to determine Full Width at Half Maximum (FWHM) for quadruple racetrack resonator.

Normalized group delay and dispersion characteristics for drop port transmittance for OQRR are shown in Figs.4(c) and (d) respectively.

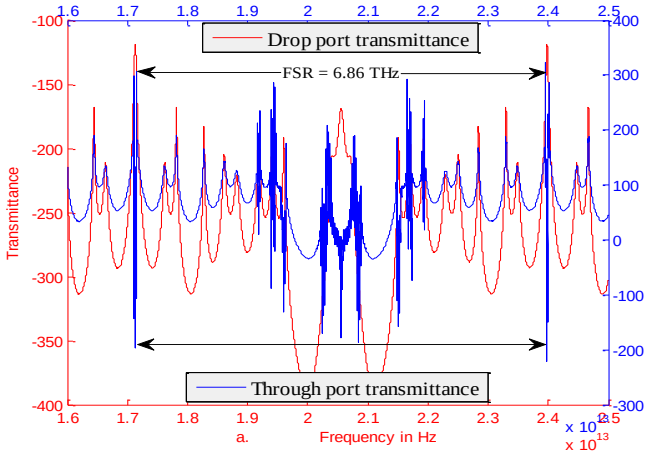

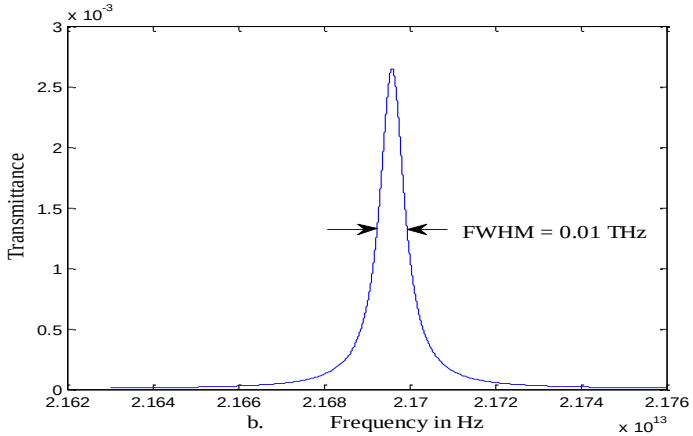

Fig 4. (a). Drop port and through the port response of an OQRR, **(b)** A zoom-in view of a single peak at1.7THz.

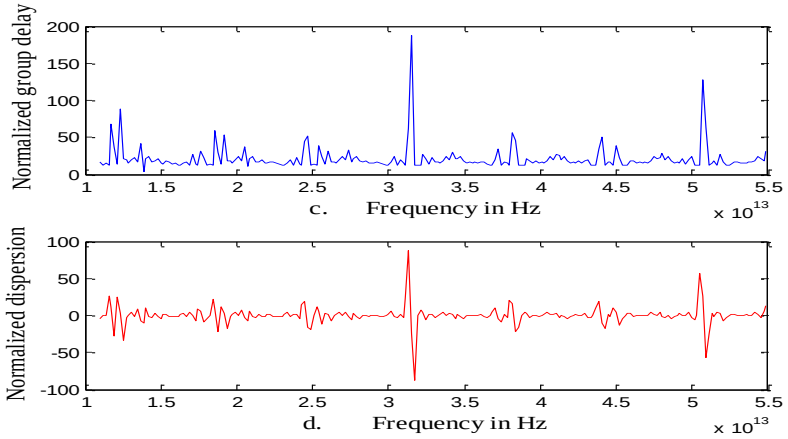

Fig 4 (c). Normalized group delay and **(d).** normalized dispersion for OQRR.

Here it is observed in Fig. 4 (c) and (d) that the normalized group delay and resulting dispersion are most prominent around the resonant peaks of the frequency response for OQRR. In other values of a frequency other than the peaks, it is seen that the group delay is minimum, and dispersion characteristics are almost flat.

V. Conclusion and Discussion

The series-coupled optical double racetrack resonator (ODRR) and optical quadruple racetrack resonator (OQRR) have been designed and analyzed based on the Vernier principle and delay line signal processing technique in Z-domain. SOI changes its group refractive index following equation (1) and is effective in fabricating this structure in a relatively smaller dimension and mitigating bending loss. As the regions of interconnections have been extended here, surface loss and dispersion loss are both taken into account. Here optical path length through the race tracks and the coupling coefficients (k_i) determine the optimum transmission characteristics at the drop and through ports. In the case of experimental double

racetrack resonator coupling coefficients between the resonators and the input/output bus waveguides are considered to be equal for optimum transmission at the drop port and the through port. FSR obtained from this architecture is 4.87 THz, which agrees well with the experimental results [XIII].

Following a similar methodology, an extended FSR of 5.77 has been obtained with superior parameters. Again this technique has been applied for analyzing higher-order racetrack resonators where we obtained a much enhanced FSR of 6.86THz compared to a similar kind of architecture [XIV]. Interstitial spurious transmission is about -100dB and is uniform over the entire frequency range with negligible resonance loss. This is very useful in communication engineering using the WDM technique to accommodate a large number of channels. FWHM obtained from one such resonant peak of OQRR is 0.01THz and the resulting Finesse is approximately 686 which is considerably high.

Group delay and *dispersion* are prominent around the resonant peaks as shown in the results. Here positive group delay is obtained and this device can also be used as an optical delay line. The results obtained for both the ODRR and OQRR are operating in the terahertz range including the C-band of the International Telecommunication Union - ITU which is useful for future communication networks. Moreover, the optical resonator-based filters are very useful for obtaining the nanophotonic devices coupled in Photonic Integrated Circuits (PIC). Racetrack resonators on silicon platforms can be molded for obtaining electro-optic modulators and submicron silicon photonic wires for on-chip optical interconnects for higher orders of resonators.

Appendix:

Loop transmittance of all individual loops:

$$L_1 = C_1 C_2 z^{-M} \quad \text{(A1)}$$

$$L_2 = C_2 C_3 z^{-N} \quad \text{(A2)}$$

$$L_3 = C_3 C_4 z^{-O} \quad \text{(A3)}$$

$$L_4 = C_4 C_5 z^{-P} \quad \text{(A4)}$$

$$L_5 = C_1.\sqrt{z^{-N}}.-jS_2.\sqrt{z^{-M}}.C_3.\sqrt{z^{-M}}.-jS_2.\sqrt{z^{-N}} = -C_1 C_3 S_2^2 z^{-(M+N)} \quad \text{(A5)}$$

$$L_6 = -C_2 C_4 S_3^2 z^{-(N+O)} \quad \text{(A6)}$$

$$L_7 = -C_3 C_5 S_4^2 z^{-(O+P)} \quad \text{(A7)}$$

$$L_8 = C_1 C_4 S_2^2 S_3^2 z^{-(M+N+O)} \quad \text{(A8)}$$

$$L_9 = C_2 C_5 S_3^2 S_4^2 z^{-(N+O+P)} \quad \text{(A9)}$$

$$L_{10} = -C_1 C_5 S_2^2 S_3^2 S_4^2 z^{-(N+M+O+P)} \quad \text{(A10)}$$

Transmittance of all possible combinations of two non touching loops:

$$L_{12} = C_1 C_3 C_2^2 z^{-(M+N)} \quad \text{(A11)}$$

$$L_{23} = C_2 C_4 C_3^2 z^{-(N+O)} \quad \text{(A12)}$$

Sabitabrata Dey

$$L_{34} = C_3 C_5 C_4^2 z^{-(O+P)} \quad \text{(A13)}$$

$$L_{31} = C_1 C_2 C_3 C_4 z^{-(M+O)} \quad \text{(A14)}$$

$$L_{41} = C_1 C_2 C_4 C_5 z^{-(M+P)} \quad \text{(A15)}$$

$$L_{42} = C_2 C_3 C_4 C_5 z^{-(N+P)} \quad \text{(A16)}$$

$$L_{54} = -C_1 C_3 C_4 C_5 S_2^2 z^{-(M+N+P)} \quad \text{(A17)}$$

$$L_{53} = -C_1 C_4 C_3^2 S_2^2 z^{-(M+N+O)} \quad \text{(A18)}$$

$$L_{61} = -C_1 C_4 C_2^2 S_3^2 z^{-(M+N+P)} \quad \text{(A19)}$$

$$L_{64} = -C_2 C_5 C_4^2 S_3^2 z^{-(N+O+P)} \quad \text{(A20)}$$

$$L_{71} = -C_1 C_2 C_3 C_5 S_4^2 z^{-(M+O+P)} \quad \text{(A21)}$$

$$L_{72} = -C_2 C_5 C_3^2 S_4^2 z^{-(N+O+P)} \quad \text{(A22)}$$

$$L_{75} = C_1 C_5 C_3^2 S_2^2 S_4^2 z^{-(M+N+O+P)} \quad \text{(A23)}$$

$$L_{84} = C_1 C_5 C_4^2 S_2^2 S_3^2 z^{-(M+N+O+P)} \quad \text{(A24)}$$

$$L_{91} = C_1 C_5 C_2^2 S_3^2 S_4^2 z^{-(M+N+O+P)} \quad \text{(A25)}$$

Transmittance of all possible combinations of three non touching loops:

$$L_{123} = C_1 C_4 C_2^2 C_3^2 z^{-(M+N+O)} \quad \text{(A26)}$$

$$L_{124} = C_1 C_3 C_4 C_5 C_2^2 z^{-(M+N+P)} \quad \text{(A27)}$$

$$L_{134} = C_1 C_2 C_3 C_5 C_4^2 z^{-(M+O+P)} \quad \text{(A28)}$$

$$L_{234} = C_2 C_5 C_3^2 C_4^2 z^{-(N+O+P)} \quad \text{(A29)}$$

$$L_{534} = -C_1 C_5 C_3^2 C_4^2 S_2^2 z^{-(M+N+O+P)} \quad \text{(A30)}$$

$$L_{614} = -C_1 C_5 C_2^2 C_4^2 S_3^2 z^{-(M+N+O+P)} \quad \text{(A31)}$$

$$L_{712} = -C_1 C_5 C_2^2 C_3^2 S_4^2 z^{-(M+N+O+P)} \quad \text{(A32)}$$

Transmittance of all four non touching loops:

$$L_{1234} = C_1 C_5 C_2^2 C_3^2 C_4^2 z^{-(M+N+O+P)} \quad \text{(A33)}$$

Conflicts of Interest:

The authors declare that they have no conflicts of interest regarding the paper.

References

I. A. Wirth L, M.G da Silva, D.M.C Neves, A.S.B Sombra, "Nanophotonicgraphene-basedracetrack- resonatoradd/drop filter", Optics Communications, 366(2016) 210-220, Elsevier.

II. A. Oppenheim, R. Schafer, "Digital Signal Processing", 2nd edition Prentice-Hall, IncEnglewood, NJ, 1975.

III. Christi K.Madsen, Jian H Zhao, "Optical filter design and analysis, A signal processing approach", John Wiley & sons, Inc, New York, 1999.

IV. D. Marcuse, "Bending losses of the asymmetric slab waveguide," *Bell System Tech. J.* **50** (8), 2551–2563 (1971).

V. Fengnian Xia, Lidija Sekaric and Yurii A. Vlasov," Mode conversion losses in silicon-on-insulator photonic wire based racetrack resonators", 1 May 2006, Vol. 14, No. 9, Optics Express.3872.

VI. H. Liu, C. F. Lam, and C. Johnson, "Scaling Optical Interconnects in Data center Networks Opportunities and Challenges for WDM," *2010 18th IEEE Symp. High Perf. Interconnects*, pp. 113–16.

VII. Intel Silicon Innovation: Fueling New Solutions for the Digital Planet, www.intel.com/technology/silicon.

VIII. J. T. Robinson, L. Chen, and M. Lipson, "On-chip gas detection in silicon optical microcavities," *Opt. Express*, vol. 16, pp. 4296–4301, March 2008.

IX. Landobasa Y.M. Tobing, Dumon Pieter, "Fundamental principles of operation and notes on fabrication of photonic microresonators, Photonic Microring Research and Application", 156, Springer, 2010 chap-1.

X. Otto Schwelb, „Transmission, Group Delay, and Dispersion in Single-Ring Optical Resonators and Add/Drop Filters- A Tutorial Overview", IEEE journal of Lightwave technology 22 (5) (2004).

XI. P. W. Coteus J. U. Knickerbocker, C. H. Lam, Y. A. Vlasov, "Technologies for exascale systems", IBM J. Res. & Dev. Vol. 55 No. 5 Paper 14 September/October 2011.

XII. R. Boeck, W. Shi, L. Chrostowski, N.A.F Jaeger, "FSR-Eliminated Vernier racetrack Resonators using Grating-Assisted Couplers", IEEE Photonics journal, DOI: 10.1109/JPHOT.2013.2280342, IEEE.

XIII. Robi Boeck, Nicolas A. F. Jaeger, Nicolas Rouger, Lukas Chrostowski "Series-coupled silicon racetrack resonators and the Vernier effect: theory and measurement" Optics Express (2010). OCIS codes: (130.0130) Integrated optics; (130.7408) Wavelength filtering devices; (230.5750) Resonators.

XIV. Robi Boeck, Jonas Flueckiger, Nicolas Rouger, Lukas Chrostowski " Experimental performance of DWDM quadruple Vernier racetrack resonators " OSA (2013) OCIS codes (230.7408) Wavelength filtering devices; (230.5750) Resonators.

XV. S.J Mason, "Feedback Properties of Signal Flow Graphs," *Proc.* IRE, Vol. 44, no. 7, pp. 920-926, July 1975.

XVI. S. Dey, S. Mandal, "Modeling and analysis of quadruple optical ring resonator performance as optical filter using Vernier principle", Optics Communications 285 (2012) 439–446.

XVII. Sabitabrata Dey, S.Mandal, " Wide free-spectral-range triple ring resonator as optical filter," Optical Engineering, SPIE,Vol. 50(8),pp 084601-(1-9), August, 2011.

XVIII. Yurii A. Vlasov, "Silicon CMOS-Integrated Nano-Photonics for Computer and Data Communications Beyond 100G", IEEE Communications Magazine, February 2012.